Further Studies of a Cold Eddy on the Eastern Side of the Gulf Stream Using Satellite Data and Ship Data

FRED M. VUKOVICH AND BOBBY W. CRISSMAN

Research Triangle Institute, P. O. Box 12194, Research Triangle Park, NC 27709

(Manuscript received 16 September 1977, in final form 13 April 1978)

ABSTRACT

A cold eddy was observed in late March and early April 1975 to encounter the eastern boundary of the Gulf Stream and entrain warm Gulf Stream water into its outer fringes. Available evidence indicated that the entrainment of Gulf Stream water in the western and southern portions of the eddy enhanced the density stratification creating available potential energy which led to an increase in kinetic energy in those regions. A secondary, cold perturbation with a high-salinity core was detected south of the center of the cold eddy. It was not clear from the data whether the conversion of available potential energy into kinetic energy increased the kinetic energy of the cold eddy, produced the secondary perturbation, or both.

1. Introduction

A Gulf Stream ring, or cold eddy, is a cyclonic circulation system consisting of a cold, less-saline central core and a warm, more-saline ring of Gulf Stream water. Evidence suggests that the cold core may at times extend to depths as great as 3000 m. Data presented by Fuglister (1971) suggests that about five to eight rings form each year. It appears from his study that the formation of rings was associated with large meanders of the north wall of the Gulf Stream (600–800 km wavelengths). A portion of the meander breaks off, crosses the Gulf Stream, and moves into the Sargasso Sea.

Generally, these eddies move south and west near the eastern boundary of the Gulf Stream. Some of these eddies, at times, encounter the eastern boundary of the Gulf Stream. Then warm Gulf Stream water is entrained into the outer fringes of the eddy reinforcing the warm ring (Vukovich, 1976). The entrainment of warm, more-saline Gulf Stream water should intensify the density contrast in the cold eddy and should affect the energetics of the eddy. This study endeavors to investigate this phenomenon.

Available evidence does not offer any information on the genesis or movement of the eddy to be studied prior to March 1975 when it was first observed by the NOAA 4 radiometers. It was located at approximately 31.5°N, 74.0°W on 26 March. The eddy moved southwestward to 31.25°N, 75.25°W on 8 April. The satellite data showed no indications of the presence of this cold eddy after late April 1975.

On 8 April 1975, the Cape Fear Technical Institute's R/V *Advance II* was sent into the region of the eddy to collect *in situ* data along two transects. The positions of the transects relative to the cold eddy are shown in Fig. 2.

2. Satellite sea surface temperature analysis

The 26 March and 8 April 1975 digitized satellite data were used to analyze the sea surface temperature distribution in the Gulf Stream ring. These data were received from NOAA uncalibrated. In order to calibrate them, the isotherm interval established by the National Environmental Satellite Service (~1°C) was assumed correct. The value of one of the isotherms was determined for the 8 April data using surface temperature data collected in the cold eddy by the *Advance II*. The temperature versus digital count was held constant and applied to the 26 March data.

Fig. 1 gives the sea surface temperature analysis off the southeast coast of the United States for 26 March 1975. The cold eddy was located, as indicated earlier, at approximately 31.5°N, 74.0°W. The surface temperature in the cold core of the ring was less than 20°C. There was a tongue of warm water to the south and east of the cold core that originated from the Gulf Stream and encircled the eddy in a cyclonic sense. Warm tongues of this nature have been discussed earlier by Vukovich (1976). West and south of the center of the cold eddy, the temperature in the warm tongue was in excess of 22°C. To the east of the center, the temperature was between 20 and 21°C. The satellite data indicated that the warm tongue did not extend completely around the eddy.

There was a secondary cold perturbation in the form of a cold lens southwest of the center of the eddy in the warm tongue, which appears connected

0022-3670/78/0838-0845$05.00

to the cold eddy. The connection arises due to smoothing required for the analysis. In the unsmoothed data, the perturbation is more in the form of a lens. The temperature in this perturbation, according to the smooth data, was between 20 and 21°C. Secondary cold perturbation associated with cold eddies have been noted earlier (Vukovich, 1976).

The cold eddy was elliptic in shape with the major axis oriented northwest to southeast. Considering the area enclosed by the 20°C isotherm, the major axis was approximately 180 km and the minor axis, 125 km.

Clouds obscured most of the sea surface on 8 April 1975 (Fig. 2). However, some pertinent information was available from the NOAA 4 sea surface temperature analysis. The data indicated that the eddy was then located at 31.25°N, 75.25°W. The average speed of the eddy was 10.7 km day^{-1} between 26 March and 8 April. The temperature in the central cold core of the eddy remained less than 20°C. The western and southern portions of the warm tongue were still present. However, the temperature in the tongue appears to have decreased in the areas south of the center of the perturbation. In the west, the temperature in the tongue was approximately 22°C, whereas in the south, the

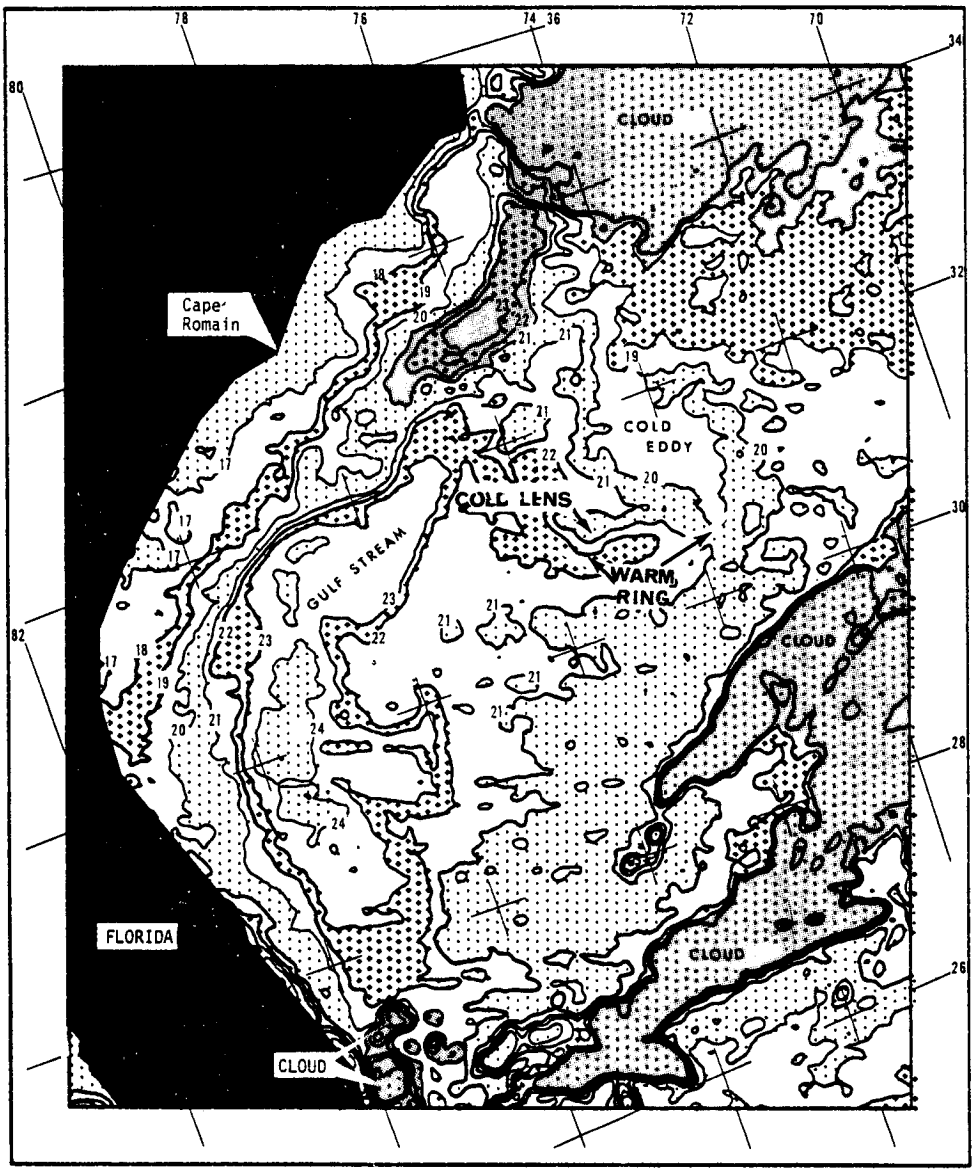

FIG. 1. Sea-surface temperature analysis (°C) using NOAA 4 VHRR data for 26 March 1975. Shaded regions indicate clouds. The stipling is used to discriminate temperature increments.

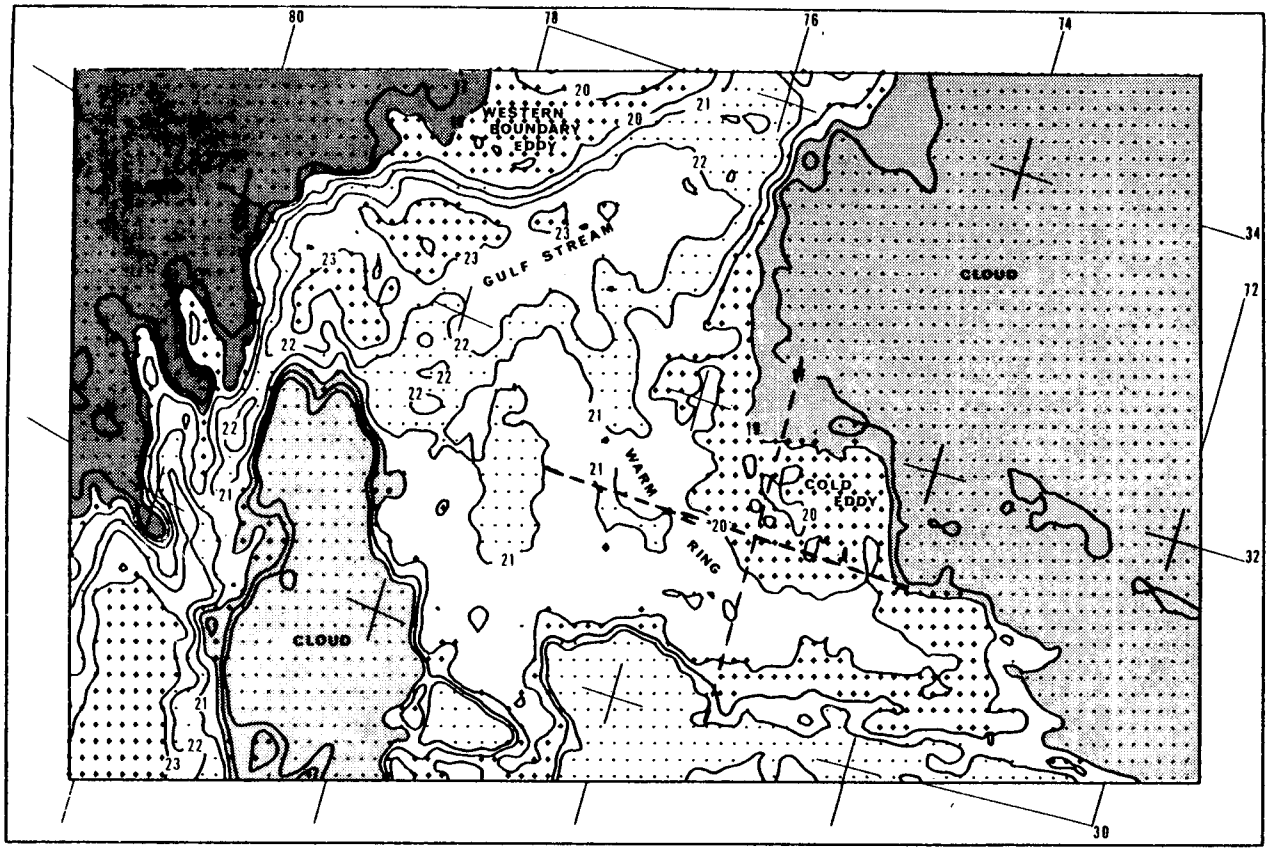

FIG. 2. Sea-surface temperature analysis (°C) using NOAA 4 VHRR data for 8 April 1975. The two transects performed by the R/V *Advance II* are also indicated (dashed line). Shaded regions indicate clouds. The stipling is used to discriminate temperature increments.

temperature was between 20 and 21°C, which was approximately a 1°C decrease from that found on 26 March in that region. The portion of the warm tongue found to the east of the center of the eddy on 26 March was barely evident due to the clouds. The presence of small lenses of warm water ($20°C < T < 21°C$) near the center of the cold eddy suggested that mixing had taken place between the warm tongue and the central core of the cold eddy. The fact that the secondary cold lens found on 26 March was no longer evident was another indication that surface mixing had taken place.

The eddy remained elliptic in shape with the major axis oriented northwest to southeast. Relative to the 20°C isotherm, the major axis was again 180 km. Because clouds obscured the eastern portions of the cold eddy, the minor axis could not be determined.

3. Physical characteristics

The temperature and salinity cross sections along the west to east and south to north transects shown in Fig. 2 are given in Fig. 3–6. The west to east transect was along 31.25°N extending from 77 to 74°W, and the south to north transect was along 75.25°W from 30 to 32.3°N. Sixteen stations about 19 km apart were accomplished along the west to east transect in the period 0115 EST 9 April 1975 to 0450 EST 10 April 1975. Fifteen stations along the south to north transect were accomplished in the period 0915 EST 10 April to 0403 EST 11 April.

One major feature in these analyses is the cold dome and the dome of low salinity associated with the cold eddy centered at 75.25°W, 31.25°N. These analyses indicate that the warm water which the satellite data indicated was being entrained from the Gulf Stream, has wrapped completely around the Gulf Stream ring at this time. This was not the case in the 26 March analyses of the satellite data. Clouds obscured the 8 April IR image analysis so that this could not be determined using these satellite data.

Table 1 indicates some statistics on the warm water in the warm ring around the cold eddy. The warm entrainment initiated on the western side of the eddy where the highest temperatures and maximum depths are indicated. The entrainment occurs in a cyclonic sense so that the southern portions of the eddy would be affected after the western portions, followed by the eastern and northern

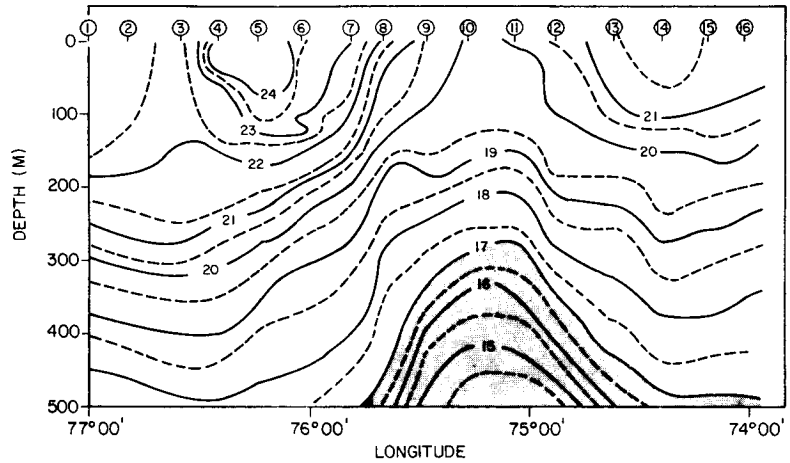

FIG. 3. Vertical temperature (°C) cross section along the west-east transect. The integration period was from 0115 EST 9 April 1975 to 0450 EST 10 April 1975. Station numbers are given at the top of the figure.

portions. As the water circulated around the eddy, both the temperature and the depth of the warm water decreased, indicating the effects of mixing.

The other major feature in the analysis is the secondary cold perturbation centered south of the center of the cold eddy at 30.67°N, 75.25°W. It should be noted that the exact position of the center of the secondary perturbation cannot be determined from these data since data were not obtained in the southwestern and southeastern quadrants. It can only be indicated that the center was south of the center of the cold eddy. The data indicated that there was an extension of the cold perturbation toward the west of the center of the cold eddy. The location of this perturbation nearly coincides with that found by Vukovich (1976) in another cold eddy. The perturbation extended through the layer from 50 to 350 m.

Furthermore, a zone of high salinity in the layer essentially from the surface to 450 m completely encircles the cold eddy. The maximum salinity and the depth of the maximum salinity in the zone is given in Table 2. The highest salinity in the zone is found in a location identical with the position of the center of the secondary cold perturbation. As in the case of the secondary cold perturbation, the highest salinity in the high-salinity zone has a well-defined extension to the west side of the eddy.

4. Dynamic characteristics

Ship drift data were also obtained along various points on the west-east and south-north transects.

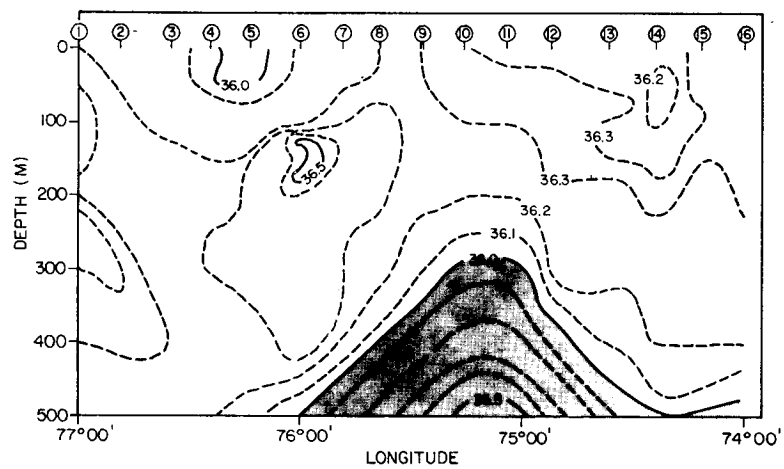

FIG. 4. Vertical salinity (‰) cross section along the west-east transect. The integration period was from 0115 EST 9 April 1975 to 0450 EST 10 April 1975. Station numbers are given at the top of the figure.

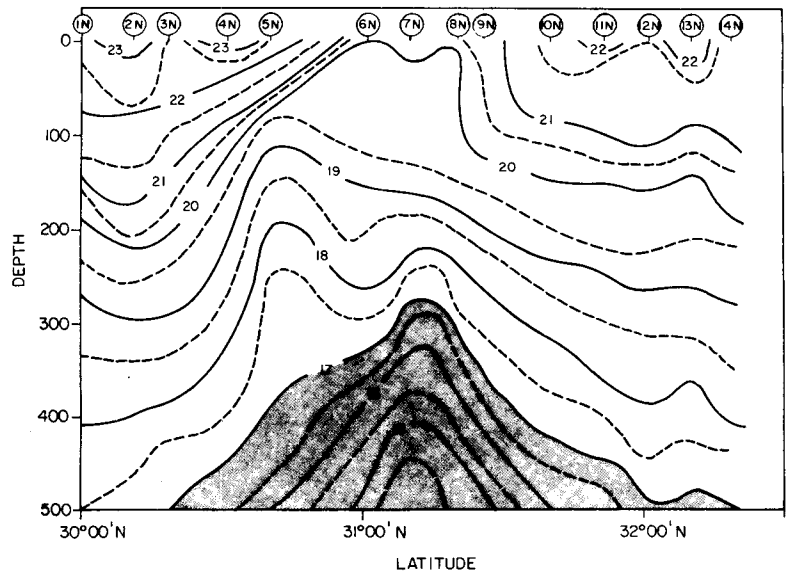

FIG. 5. Vertical temperature (°C) cross section along the south-north transect. The integration period was from 0915 EST 10 April 1975 to 0403 EST 11 April 1975. Station numbers are given at the top of the figure.

Table 3 gives average current speeds and directions at the surface derived from the ship drift observations in various sectors of the cold eddy. The ship drift observations indicated that the strongest currents were on the western side of the eddy and were directed to the southeast. Sizeable currents were found to the south and east of the cold eddy and were directed to the north-northeast. The speed of the current in the southern section was larger than that in the eastern section. The currents north of the eddy were weak and there was no indication of westward flow in this region, which should occur in true cyclonic motion.

Figs. 7 and 8 yield the analysis of the geostrophic currents computed relative to the 450 m depth from the data available along the west-east and south-north transects. Fig. 9 summarizes the circulation established from the computations of geostrophic current. The figure yields the dynamic topography at the 200 m depth, relative to the 450 m depth. The

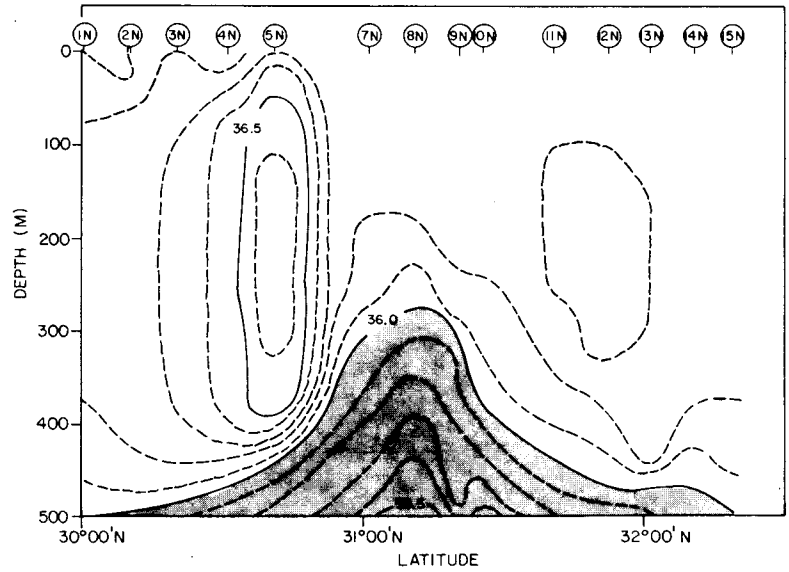

FIG. 6. Vertical salinity (‰) cross section along the south-north transect. The integration period was from 0915 EST 10 April 1975 to 0403 EST 11 April 1975. Station numbers are given at the top of the figure.

TABLE 1. Various statistics concerning the entrainment of warm Gulf Stream water around the cold eddy derived from the transect data.

Location of center of warm water entrainment	Maximum temperature at the surface (°C)	Maximum depth of 20°C isotherm (m)
West of center of cold eddy	24	300
South of center of cold eddy	23	225
East of center of cold eddy	22	175
North of center of cold eddy	22	150

figure shows that the cold eddy was characterized by a general cyclonic rotation, with the strongest currents to the west and south of the eddy's center (the maximum geostrophic current west of the center of the eddy at the surface was 85 cm s^{-1} and was flowing to the south, and the maximum geostrophic current south of the center of the cold eddy at the surface was 100 cm s^{-1} and was flowing to the east). The analysis shows two centers of cyclonic motion. The first center was located at 75.25°W, 31.25°N and correlated with the thermal center of the cold eddy. The second cyclonic center was located at 75.25°W, 30.67°N and correlated with the center of the second thermal-salinity perturbation. There was strong anticyclonic shear separating the two cyclonic centers.

5. Energy characteristics

The characteristics of available potential energy and kinetic energy along each transect were studied. In order to determine the available potential energy, the anomaly P' of potential energy per unit area was computed (Fofonoff, 1962), i.e.,

$$P' = (1/g) \int_p p\delta \, dp, \tag{1}$$

where p is pressure, g the acceleration of gravity, and δ the specific anomaly.

The anomaly of potential energy was computed relative to the 450 m depth. The available potential energy along each transect was also computed relative to the 450 m depth and with respect to a reference value established from data in the Sargasso Sea.

The kinetic energy was determined using the computed geostrophic currents relative to the 450 m depth. Along the west-east transect, the south-north component K_y of the kinetic energy was computed from

$$K_y = (1/g) \int_p c_y^2 dp, \tag{2}$$

TABLE 2. The depth of and the maximum salinity in the high-salinity zone relative to the center of the eddy.

Location	Maximum salinity (‰)	Depth of maximum salinity (m)	Latitude (°N)	Longitude (°W)
West of eddy	36.60	150	31.25	76.00
South of eddy	36.65	175	30.67	75.25
East of eddy	36.30	150	31.25	74.88
North of eddy	36.30	175	31.85	75.25

where c_y is the south-north component of the geostrophic current.

The west-east component of the kinetic energy K_x was computed using

$$K_x = (1/g) \int_p c_x^2 dp, \tag{3}$$

where c_x is the west-east component of the geostrophic current.

Fig. 10 gives the distribution of available potential energy along the two transects, and Fig. 11 the distribution of kinetic energy. The solid line represents the west-east transect data, and the dashed line, the south-north transect data. It should be noted that low available potential energy and high kinetic energy relative to the center of the cold eddy were found to the west, south, north and east. The highest kinetic energy was found in the southern portions of the eddy, though the kinetic energy in the western portions was considerably higher than that found in the northern and eastern portions of the eddy. The zone of maximum kinetic energy west and south of the center of the cold eddy was located about 85 km from that center. However, the minor zones of maximum kinetic energy found to the east and north of the center of the cold eddy were located between 10 and 25 km from the center.

The largest value of available potential energy along the west-east transect was found at the center of the cold eddy. However, along the south-north transect, the maximum value was located at the center of the secondary perturbation. This was the

TABLE 3. Average speeds and direction of surface currents estimated from ship drift observations. Averages were computed from observations made along the transects along a line entering 60 km from the center of the cold eddy (75.25°W, 31.25°N) in the direction of interest.

Location relative to the center of eddy	Average speed (ms^{-1})	Direction to which current is flowing	Number of observations used to compute average
West	2.1	SE	3
South	1.5	NNE	3
East	1.0	NNE	3
North	0.10	SSE	2

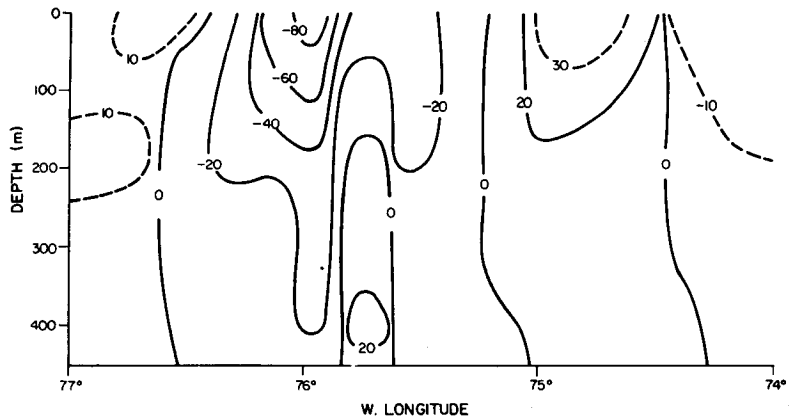

FIG. 7. Analysis of geostrophic currents (cm s^{-1}) relative to the 450 m depth along the west-east transect. Positive values indicate northward flow and negative values southward flow.

largest value along either transect. The lowest value of available potential energy appeared to be displaced upstream of the largest values of kinetic energy.

The largest values of kinetic energy were found in the western and southern portions of the eddy. The kinetic energy was considerably smaller in the eastern and northern portions which were relatively unaffected by the entrainment of Gulf Stream water. The kinetic energy in the northern and eastern portions probably represent the magnitude of that energy which would exist in the western and southern portions of the eddy had they not been affected by the entrainment. The entrainment of warm, more-saline Gulf Stream water into the western and southern portions of the cold eddy increased the density contrast (i.e., available potential energy) relative to the cold, less-saline core of the eddy. It is not clear from the data whether the conversion of available potential energy into kinetic energy, which must have followed, went into increasing the kinetic energy of the cold eddy or creating the secondary perturbation.

6. Discussion of results

A cold eddy in the Sargasso Sea encountered the eastern boundary of the Gulf Stream and the circulation of the cold eddy entrained warm Gulf Stream water into its outer fringes. The entrainment of the warm Gulf Stream water intensified the density contrast relative to the center of the cold eddy, creating a reservoir of available potential energy. The most intense mass contrasts were produced in the western and southern portions of the cold eddy. Diffusion of heat and mass and the apparent fact that the eddy did not stay at the Gulf Stream's eastern boundary for a long period of time prevented sizeable mass contrasts from being developed in the northern and eastern portions of the eddy. After 8 April the eddy was not clearly seen by the satellite until approximately 17 April. At that time the satellite data indicated that the entrainment of Gulf Stream water had ceased because the eddy had moved away from the Gulf Stream, and the temperature difference between the cold central core of the eddy at the surface and the warm ring was diminishing. After 17 April the cold eddy was not detected by the satellite's radiometers.

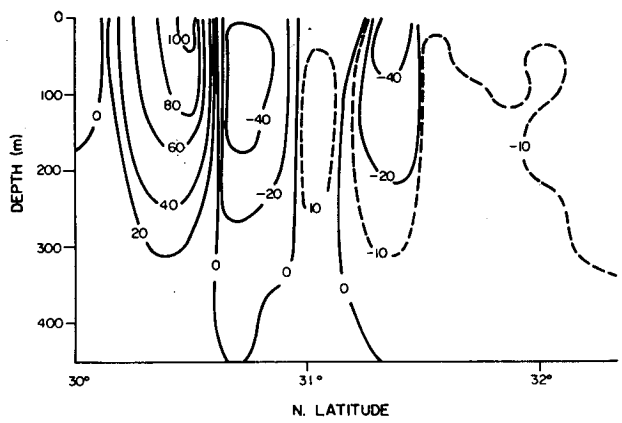

FIG. 8. Analysis of geostrophic current (cm s^{-1}) relative to the 450 m depth along the south-north transect. Positive values indicate eastward motion and negative values westward motion.

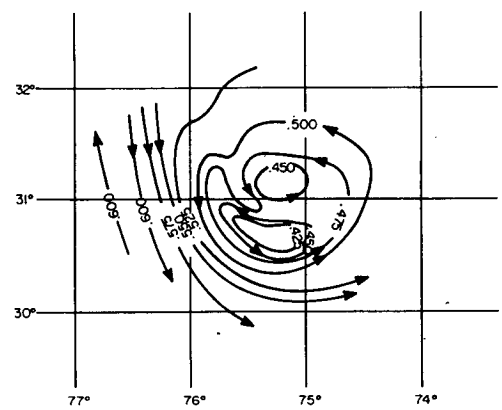

FIG. 9. Analysis of dynamic topography (dyn m) at the 200 m depth relative to the 450 m depth.

The evidence indicated that large amounts of kinetic energy were present in the western and southern portions of the cold eddy suggesting conversion of the available potential energy, created by the entrainment of Gulf Stream water, into kinetic energy. The core of maximum kinetic energy was found further from the center of the eddy in the southern and western portions of the eddy (~85 km) than in the eastern and northern portions (10–25 km) which were significantly less affected by the entrainment. It is not clear from the data whether the larger amounts of kinetic energy in the western and southern portions of the cold eddy are associated with the cold eddy, a secondary perturbation found in this region, or both.

A secondary cold perturbation having a cyclonic circulation was detected south of the center of the cold eddy. The *in situ* temperature data indicated the perturbation extends from the 50 m depth to the 350 m depth (9–11 April 1975). The 26 March 1975 satellite sea surface temperature data indicated the presence of an isolated cold lens in the middle of the entrainment of Gulf Stream water south of the center of the cold eddy and in about the same position the secondary perturbation detected in the *in situ* data. Potential sources of the cold water in the lens are either the cold eddy in which case a portion of the cold eddy was detached and possibly isolated by the entrainment process, or the subsurface in which case the cold subsurface water is advected vertically to the surface. If the cold lens at the surface detected by the satellite and the secondary cold perturbation found in the analysis of the *in situ* data are one and

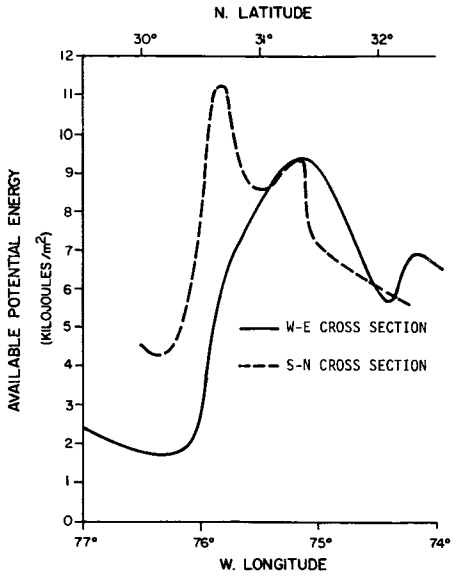

FIG. 10. The variation of available potential energy relative to the 450 m depth along the two transects.

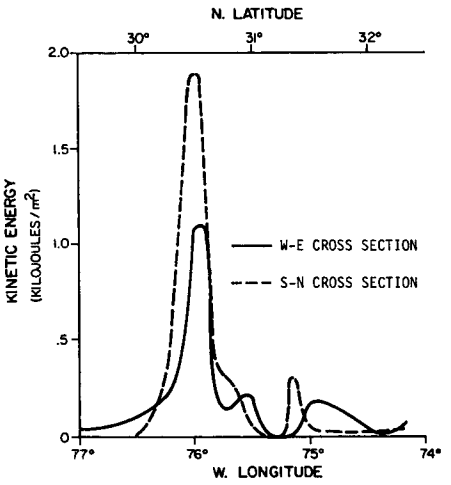

FIG. 11. The variation of kinetic energy relative to the 450 m depth along the two transects.

the same feature, then the cold lens is not a portion of the cold eddy because the secondary perturbation had a high-salinity core in contrast to the low-salinity core of the cold eddy.

The maximum salinity in the secondary perturbation was found at the 150 to 175 m depth. Since the perturbation is found in the region where there is entrainment of Gulf Stream water, it is possible that the source of the high salinity is the high-salinity core of the Gulf Stream which is normally centered at the 200 m depth and extends through a layer from about 100 to 400 m.

Acknowledgments. This research was sponsored by the National Oceanic and Atmospheric Administration/National Environmental Satellite Service under Contract 6-35263. The authors wish to acknowledge the interest and assistance of Dr. A. E. Strong and Mr. John Pritchard of NOAA/NESS. The authors also wish to express their appreciation to Captain Arthur Jordan, his staff, and the crew of the Cape Fear Technical Institute's R/V *Advance II*. We wish to thank the numerous members of the NOAA Weather Station at Rayleigh/Durham Airport for their assistance in providing weather reports and collecting orbital data for the NOAA satellite.

REFERENCES

Fofonoff, N. P., 1962: Dynamics of ocean currents. *The Sea*, Vol. 1, M. N. Hill, Ed., McGraw-Hill, 323–395.

Fuglister, F. C., 1971: Cyclonic rings formed by the gulf stream. *Studies in Physical Oceanography, A Tribute to Georg Wust on his 80th Birthday*, A. Gordon, Ed., Gordon and Breach, 137–168.

Vukovich, F. M., 1976: An investigation of a cold eddy on the eastern side of the Gulf Stream using NOAA 2 and NOAA 3 satellite data and ship data. *J. Phys. Oceanogr.*, **6**, 605–612.